Proceedings of the Sixth International Conference on
Railway Technology: Research, Development and Maintenance
Edited by: J. Pombo
Civil-Comp Conferences, Volume 7, Paper 22.2
Civil-Comp Press, Edinburgh, United Kingdom, 2024
ISSN: 2753-3239, doi: 10.4203/ccc.7.22.2

Development of an Extended Kalman Filter for Determination of the Normal Wheel-Rail Contact Force

B. De Leeuw[1,2], Z. Yang[1] and Z. Li[1]

[1] Faculty of Civil Engineering and Geosciences, Delft University of Technology, Netherlands
[2] Asset Management, ProRail, The Netherlands

Abstract

The estimation of railway friction level requires an accurate determination of the wheel-rail contact force. This study developed an extended Kalman filter to estimate the normal wheel-rail contact force. The filter is based on a dynamic system, taking both the axlebox acceleration and vertical primary suspension force as the main input variables. The multi-body dynamics simulation results, including the simulated axle-box acceleration, primary suspension force and wheel-rail contact force, were then used to tune and validate the extended Kalman filter. The study indicates the extended Kalman filter, is reliable for estimating the normal wheel-rail contact force. To determine the sensitivity of the filter, the effect of the vehicle speed was examined. The study shows the accuracy of the extended Kalman filter may decrease with the increase in the running speed of the vehicle. By tuning the filter based on a high running speed, the proposed extended Kalman filter is promising for the determination of the normal wheel-rail contact force in practice.

Keywords: multi-body dynamics simulation, extended Kalman filter, vehicle-track interaction, normal wheel-rail contact force, axle-box acceleration, primary suspension force

1 Introduction

The interaction between wheel and rail is a critical factor for the operation of rail traffic. Since trains heavily rely on the friction between wheel and rail for acceleration and braking, the coefficient of friction (CoF) is a crucial aspect of this interaction. The CoF has several correlations to the safety and reliability of rail traffic operation, including affecting the acceleration and braking performance of a rail vehicle, and wear of the wheel and rail which causes derailment risk and temporary speed reductions. Therefore, infrastructure managers and train operators aim to control the CoF appropriately. Before being able to control the CoF it is important to know the CoF. This has proven to be a challenge since this value depends on factors like humidity, surface roughness and rolling velocity. In the past, different devices have been used to measure the CoF, like a hand-pushed tribometer [1] or low-speed vehicle [2]. One of the first attempts at train-borne measurements was performed by British Rail in 1972. Despite having the advantage of not having to scale the wheel-rail contact forces, it was only possible to compute the CoF at the point of wheel sliding [3, 4]. Popovici [3] showed experimentally using a simple sliding sensor can be successful for the detection of friction levels, but the system is sensitive to abrasion and developed heat during long-term use. It is thus crucial to develop an accurate and reliable device for determining the CoF that can account for various scenarios in rail traffic operation.

The CoF can be determined by measuring the wheel-rail contact forces. Since the adhesion coefficient (AC) is bounded by the CoF, the CoF can be represented as the maximum AC. The AC(μ_a) represents the ratio between the magnitudes of the tangential wheel-rail contact forces(F_T) and the normal wheel-rail contact force(F_N) [5].

$$\mu_a = \frac{F_T}{F_N} \tag{1}$$

To calculate the AC, it is necessary to determine the tangential and normal wheel-rail contact forces. Direct methods, such as using strain gauges on instrumented wheelsets, can be used to measure these forces [6]. However, these methods are often expensive and complicated to implement on in-service passenger vehicles. Therefore, using an indirect method for determining the normal wheel-rail contact force may be a more promising approach.

One possible indirect method for determining wheel-rail contact forces is to use vehicle responses. Several approaches exist for processing the vehicle responses and obtaining the contact forces, such as using an inverse wagon model [7] or applying a Kalman filter (KF). This method has been proposed in several papers, including Zhang et al. [8],Mal et al. [9], and Strano and Terzo [10]. However, these papers only determine the creep forces or calculate the CoF. In these papers, the CoF is calculated based on a given normal wheel-rail contact force, which either comes from multibody dynamics simulation (MBS) or the vertical primary suspension force. However, an inaccurate normal wheel-rail contact force has an impact on the CoF and AC calculation. The accurate determination of the normal wheel-rail contact force should thus be investigated.

This paper develops an indirect method for the determination of the normal contact force. The indirect methods can be split into two categories, namely forward wagon models and inverse wagon models. A forward wagon model uses track irregularities and vehicle speed to get the vehicle responses [7]. Naeimi et al. [11], proposed a 3D dynamic model to obtain the wheel-rail contact forces. It considered multiple track irregularity cases, whereby the irregularities were the input for the numerical model of the vehicle. Meli et al. [12] developed a similar model for real-time application. It was found that although the model works, and can be validated against available MBS models, the development of the real-time model has to find a compromise between accuracy and efficiency due to the complexity of the numerical models and their integration times. The forward wagon model is often built up in MBS software, like VI-Rail, SIMPACK or Vampire.

Another indirect method is called the inverse wagon model. This model uses the vehicle dynamic responses, like the acceleration of the car body or bogie, to determine the wheel-rail contact forces. Xia, Bleakley, and Wolf [13] developed an inverse wagon model which determined the lateral and vertical contact forces only using the measurements of the car body responses ([7]). Sun, Cole, and Spiryagin [14] also used a two-dimensional inverse wagon model to determine the secondary suspension, primary suspension and wheel-rail contact forces based on wagon components and bogie side-frame accelerations. The model was simplified to support an online application. Zhu et al. [15] proposed a different technique by using a time-domain inversion method. Instead of the vehicle body accelerations, the axleBox acceleration (ABA) is used as input conditions to determine the vertical and horizontal wheel-rail contact forces. The model was then implemented in SIMPACK for a high-speed train. A laboratory test verified the inversion model. The simulation results from SIMPACK showed a high relative precision for the operation of high-speed vehicle.

Wei et al. [16] used an inverse model for the evaluation of derailment by measuring the displacement of the primary suspension and the accelerations of the bearing box and using the relative velocities of the primary dampers and distance between nominal running cycles. Moment-balanced equations are used to identify the wheel-rail contact forces. The indirect method was verified by comparing the wheel-rail contact forces with the forces from SIMPACK. When testing the method on a high-speed passenger car, running at 60 km/h, the error was not higher than 10%. Ronasi and Nielsen [17] concluded using an inverse method, although accurate, comes with a significant computational cost. This makes the inverse method less suitable for processing in real-time.

To accurately calculate the AC, an accurate estimation of this normal wheel-rail contact force needs to be considered. Combining the use of the primary suspension force and ABA, with an extended Kalman filter (EKF), could give an accurate estimation of the normal wheel-rail contact force. This paper proposes an indirect train-borne measurement of the normal wheel-rail contact force, using the vertical primary suspension force (VPSF) and the vertical ABA. These vehicle responses are processed by an EKF to predict the normal wheel-rail contact force.

2 Methodology

To evaluate the accuracy of the EKF its output is compared with the output of MBS. The EKF is built up based on a force determination model.

2.1 Force determination model

This force determination model is based on a vehicle model consisting of a car body and two bogies. For the EKF the normal wheel-rail contact force, adjusted from Knothe and Stichel [18], is expressed as:

$$F_N = m_w * ABA + m_w * g + F_{PS} \tag{2}$$

Whereby:

$F_N =$	Normal wheel-rail contact force
$m_w =$	Mass of wheel
$ABA =$	Axlebox acceleration in vertical direction
$g =$	Gravitational acceleration
$F_{PS} =$	Vertical primary suspension force

2.2 Extended Kalman filter

The system defined in the previous section is then used as the input for the EKF. The EKF is, in the railway field, used as an estimator of unknown variables of a state-space model [19, 10]. The state-space model defines the force determination model as a set of inputs, outputs, and variables which are related by a differential equation. The EKF is defined into two steps, namely the prediction and update steps. The prediction step predicts the unknown variable at the next time step, based on the force determination model, and the current variable estimate. The update step updates the predicted unknown variable by evaluating the error between the estimate and the measurement.

2.3 Multi-body dynamics simulation & validation

The output of the EKF is compared with the normal wheel-rail contact force output of the MBS. For the simulations, the benchmark Manchester vehicle[20] of VI-Rail has been used. To evaluate the performance of the EKF effect of different vehicle speeds is compared. Before the comparison, the filter first has been tuned to get the most optimal result. This tuning is performed by adjusting the process and measurement noise, which are an input of the EKF. This tuning is performed for the vehicle running on a straight track with track irregularities with a speed of 100 km/h.

The study compares the effect of the vehicle's running speed on the performance of the EKF. It is important to evaluate the effect of the speed, since the EKF is tuned for a running speed of 100 km/h. However, in the operational phase, a vehicle does not only run at 100 km/h. Therefore, different speed inputs have been compared, ranging from 60 to 140 km/h. The speeds are tested for both a straight and curved track section. The curved section has a radius of 690 metres and an installed cant of 75 millimetres.

3 Results

In this section, the effect of the different vehicle speeds are evaluated. The evaluation is performed with a normalised histogram and statistical values, i.e. mean, median, minimum, and maximum. The histograms display the relative probability of the error and show the minimum 5^{th} percentile (P05) and maximum 95^{th} percentile (P95). For the evaluation, a P05 and P95 a value close to zero, e.g. -1 kN or 1 kN, has a better performance than a value further from zero, e.g. -10 kN or 10 kN.

Figure 1 illustrates a significant effect of the train speed on the accuracy of the EKF. Since the EKF is tuned for straight track with 100 km/h, both deviations above and under the 100 km line are shown. The figure illustrates a difference between the two minimum zero probability points. At 140 km/h, there is an error of about -4 kN, while at 60 km/h, the error is -2.5 kN. The difference between the maximum zero probability points is slightly smaller, with almost 4 kN and 3 kN respectively. Additionally, the figure illustrates the 140 km/h having both the lowest P05 and the highest P95. Both percentiles show a roughly 0.7 kN difference between the 60 km/h and 140 km/h. The 140 km/h shows an P05 error of -1.86 kN and a P95 percentile error of 2.12 kN. The error percentage at P05 and P95 from the normal wheel-rail contact force is then -2.23% and 2.53% respectively. Table 1 shows other statistic values for the speed impact on straight track.

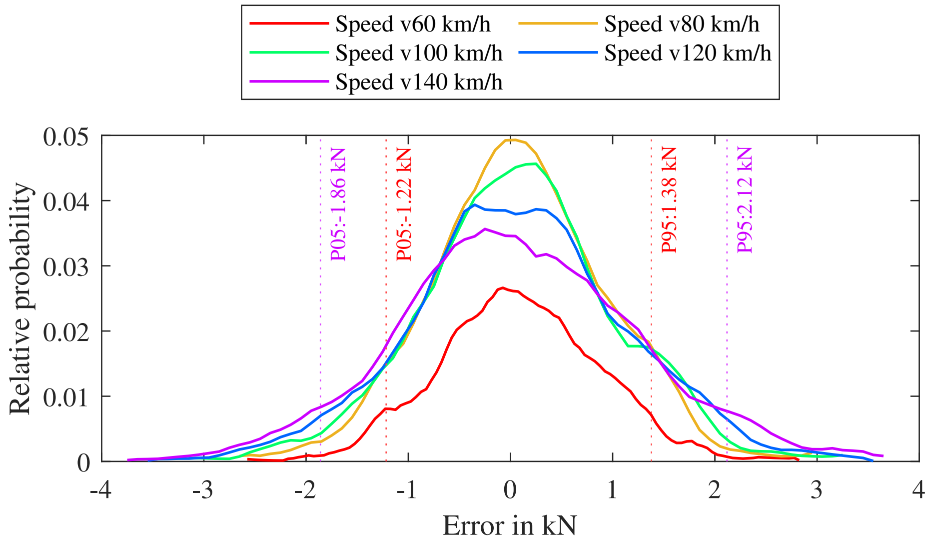

Figure 1: Distribution of normal contact force error for different running speeds - straight track.

Speed [km/h]	Mean[%]	Median[%]	Minimum[%]	Maximum[%]
60	0.21	0.12	-4.26	5.80
80	0.21	0.13	-4.29	6.28
100	0.22	0.15	-4.88	6.87
120	0.23	0.12	-5.35	7.33
140	0.22	0.03	-5.61	7.68

Table 1: Normal wheel-rail contact force error percentages for speed effect on straight track

On a curved track, speed has an even greater effect on the performance of the EKF. Figure 2 shows the relative probability of an error occurring. The figure shows a significantly wider distribution, roughly 10 kN, for 140 km/h than for 60 km/h, and a higher probability for most of the error values. In contrast to the straight track, the 140 km/h simulation does not have the highest P95, but the 60 km/h simulation has the highest P95 with a value of 2.85 kN. The error percentages at P05 and P95 from the normal wheel-rail contact force are then -15.96% and 5.26%, respectively. Table 2 shows other statistic values for the speed impact on a curved track.

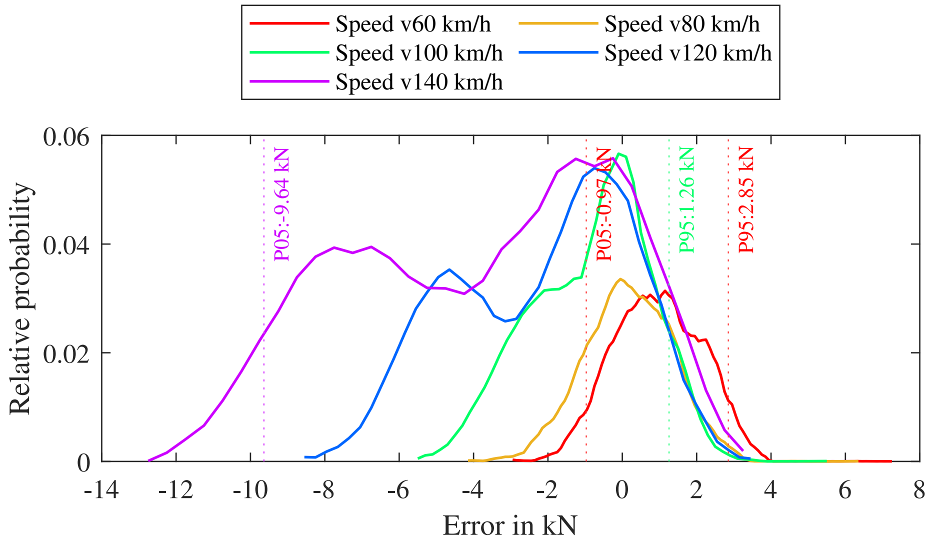

Figure 2: Distribution of normal contact force error for different running speeds - curved track.

Speed [km/h]	**Mean [%]**	**Median [%]**	**Minimum [%]**	**Maximum [%]**
60	1.86	1.77	-5.12	16.49
80	0.39	0.31	-6.64	13.57
100	-1.26	-0.96	-8.39	10.75
120	-3.07	-2.69	-11.97	7.02
140	-5.07	-4.77	-15.96	7.40

Table 2: Normal wheel-rail contact force error percentages for speed impact on curved track

It is, however, important to note that the radius and cant of the curved section have not been adjusted based on the speed. As a result, the speed effect in a curve can show higher errors than in a real curve. This is because an equilibrium force is often designed in curves by adjusting the design speed and installed cant and matching it to the curve radius.

4 Concluding remarks

This study proposed an EKF and assessed its effectiveness for the determination of the normal wheel-rail contact force. To evaluate how the EKF performs, the vehicle running speed was adjusted. The running speed has a significant effect on the performance of the EKF. Since the speed effects the performance of the EKF, it is important to tune the filter to the correct speed. For the straight track, it would be best to tune the EKF for the maximum speed of the vehicle, as lower speed cases generally perform

better than the higher speed cases. This principle can also be applied to the curved section.
To further determine the effectiveness and accuracy of the EKF a more detailed parameter study will be conducted to examine its sensitivity to other vehicle-track interaction parameters, e.g. applied traction, track stiffness, vehicle loading, and curve radius.

References

[1] Y.A. Areiza et al. "Field measurement of coefficient of friction in rails using a hand-pushed tribometer". In: *Tribology International* 82 (2015). 2013 Joint Event on Tribology in Lyon 40th Leeds-Lyon Symposium on Tribology. Leeds-Lyon at 40: is the past still present? and Tribochemistry 2013, the Satellite Forum of WTC'2013 Torino Exploring tribochemical processes, pp. 274–279. ISSN: 0301-679X. DOI: https://doi.org/10.1016/j.triboint.2014.08.009. URL: https://www.sciencedirect.com/science/article/pii/S0301679X14003041.

[2] H Harrison, T McCanney, and J Cotter. "Recent developments in coefficient of friction measurements at the rail/wheel interface". In: *Wear* 253.1 (2002). CM2000 S.I., pp. 114–123. ISSN: 0043-1648. DOI: https://doi.org/10.1016/S0043-1648(02)00090-X. URL: https://www.sciencedirect.com/science/article/pii/S004316480200090X.

[3] Radu Popovici. "Friction in wheel-rail contacts". PhD thesis. Ensched: University of Twente, Feb. 2010. ISBN: 9789036529570.

[4] D. J. Watkins. "EXPLORING ADHESION WITH BRITISH RAIL'S TRIBOMETER TRAIN". In: 1975. URL: https://api.semanticscholar.org/CorpusID:96468659.

[5] Zhen Yang et al. "An experimental study on the effects of friction modifiers on wheel–rail dynamic interactions with various angles of attack". In: *Railway Engineering Science* 30.3 (Sept. 2022), pp. 360–382. ISSN: 26624745. DOI: 10.1007/s40534-022-00285-y.

[6] Andrea Bracciali, Fosso del Cavaliere, and Mattia Macherelli. "Review of Instrumented Wheelset Technology and Applications". In: 2014. URL: https://api.semanticscholar.org/CorpusID:55820530.

[7] Fujie Xia, Colin Cole, and Peter Wolfs. "An inverse railway wagon model and its applications". In: *User Modeling and User-Adapted Interaction* 45.6 (2007), pp. 583–605. ISSN: 17445159. DOI: 10.1080/00423110601079151.

[8] Zhongshun Zhang et al. "Parameter estimation of a railway vehicle running bogie using extended Kalman filter". In: *Proceedings of the 33rd Chinese Control Conference*. 2014, pp. 3393–3398. DOI: 10.1109/ChiCC.2014.6895501.

[9] Khakoo Mal et al. "Extended Kalman filter for estimation of contact forces at wheel-rail interface". In: (Apr. 2020), pp. 279–301. DOI: 10.17993/3ctecno.2020.specialissue5.279-301.

[10] Salvatore Strano and Mario Terzo. "On the real-time estimation of the wheel-rail contact force by means of a new nonlinear estimator design model". In: *Mechanical Systems and Signal Processing* 105 (2018), pp. 391–403. ISSN: 0888-3270. DOI: https://doi.org/10.1016/j.ymssp.2017.12.024. URL: https://www.sciencedirect.com/science/article/pii/S088832701730657X.

[11] Meysam Naeimi et al. "3D dynamic model of the railway wagon to obtain the wheel-rail forces under track irregularities". In: *Proceedings of the Institution of Mechanical Engineers, Part K: Journal of Multi-body Dynamics* 229.4 (Dec. 2015), pp. 357–369. ISSN: 20413068. DOI: 10.1177/1464419314566833.

[12] Enrico Meli et al. "A railway vehicle multibody model for real-time applications". In: *Vehicle System Dynamics* 46.12 (Dec. 2008), pp. 1083–1105. ISSN: 00423114. DOI: 10.1080/00423110701790756.

[13] F Xia, S Bleakley, and P Wolf. *The estimation of wheel-rail interaction forces from wagon accelerations*. Tech. rep. 2005.

[14] Yan Quan Sun, Colin Cole, and Maksym Spiryagin. "Monitoring vertical wheel-rail contact forces based on freight wagon inverse modelling". In: *Advances in Mechanical Engineering* 7.5 (May 2015), pp. 1–11. ISSN: 16878140. DOI: 10.1177/1687814015585431.

[15] Tao Zhu et al. *Estimation of Wheel/Rail Contact Forces Based on an Inverse Technique*. Tech. rep. 2013.

[16] Lai Wei et al. "Indirect method for wheel-rail force measurement and derailment evaluation". In: *Vehicle System Dynamics* 52.12 (Dec. 2014), pp. 1622–1641. ISSN: 17445159. DOI: 10.1080/00423114.2014.953180.

[17] Hamed Ronasi and Jens C.O. Nielsen. "Inverse identification of wheel–rail contact forces based on observation of wheel disc strains: an evaluation of three numerical algorithms". In: *Vehicle System Dynamics* 51.1 (Jan. 1, 2013). Publisher: Taylor & Francis _eprint: https://doi.org/10.1080/00423114.2012.713498, pp. 74–90. ISSN: 0042-3114. DOI: 10.1080/00423114.2012.713498. URL: https://doi.org/10.1080/00423114.2012.713498 (visited on 05/16/2024).

[18] Klaus Knothe and Sebastian Stichel. "Vertical Dynamics, Equations of Motion, and Free Vibrations". In: *Rail Vehicle Dynamics*. Cham: Springer International Publishing, 2017, pp. 81–105. ISBN: 978-3-319-45376-7. DOI: 10.1007/978-3-319-45376-7_4. URL: https://doi.org/10.1007/978-3-319-45376-7_4.

[19] R. E. Kalman. “A New Approach to Linear Filtering and Prediction Problems”. In: *Journal of Basic Engineering* 82.1 (Mar. 1960), pp. 35–45. ISSN: 0021-9223. DOI: 10.1115/1.3662552. eprint: https://asmedigitalcollection.asme.org/fluidsengineering/article-pdf/82/1/35/5518977/35_1.pdf. URL: https://doi.org/10.1115/1.3662552.

[20] Simon Iwnick. “Manchester Benchmarks for Rail Vehicle Simulation”. In: *Vehicle System Dynamics* 30.3-4 (1998), pp. 295–313. DOI: 10.1080/00423119808969454. eprint: https://doi.org/10.1080/00423119808969454. URL: https://doi.org/10.1080/00423119808969454.